Synthesis, structure and polymerization behaviour of borane adducts of a phosphorus-bridged [1]ferrocenophane, $[(\eta\text{-}C_5H_4)_2FePPh]$

Chris E. B. Evans, Alan J. Lough, Hiltrud Grondey and Ian Manners*

Department of Chemistry, University of Toronto, Toronto, ON, M5S 3H6, Canada.
E-mail: imanners@chem.utoronto.ca

Received* (*in New Haven, USA*) *27th January 2000, Accepted 19th March 2000

Phosphorus(III)-bridged [1]ferrocenophanes cannot be polymerized *via* transition-metal catalyzed ring-opening polymerization, presumably due to the phosphorus lone pair ligating the catalyst. We have investigated a potential solution to this problem, which involves protection of the phosphorus lone pair through the formation of borane adducts. The adducts $[(\eta\text{-}C_5H_4)_2FeP(Ph)BX_3]$ (**2**, X = H; **3**, X = Cl) were synthesized in high yield from the reactions of appropriate boranes with *P*-phenylphospha[1]ferrocenophane, **1**, and fully characterized by NMR, UV–Vis, MS, elemental analysis, and X-ray crystallography. Ring-opening polymerizations of **2** and **3** have been attempted both thermally and using transition-metal catalysts, resulting in insoluble polymeric products, $[(\eta\text{-}C_5H_4)_2FeP(Ph)BX_3]_n$ (**5**, X = H; **6**, X = Cl), which have been characterized by solid-state NMR and by pyrolysis-MS. Well-defined borane adducts of poly(ferrocenylphenylphosphine), $[(\eta\text{-}C_5H_4)_2FeP(Ph)BX_3]_n$ (**5b**, X = H; **6b**, X = Cl) were synthesized and characterized to provide comparative data for the insoluble products **5a**, **6a** and **6c**. The data support the conclusion that both **2** and **3** may be ring-opened thermally to provide polymeric products consistent with the corresponding adducts of poly(ferrocenylphenylphosphine) **4**. In contrast, transition-metal catalyzed ROP proceeds inefficiently, leading predominantly to products of unknown structure.

Poly(ferrocenylphosphines) (*e.g.* **4**) obtained from the ring-opening polymerization (ROP) of [1]ferrocenophanes such as *P*-phenylphospha[1]ferrocenophane, **1**, have potential applications as catalytic materials based upon the reactivity of the phosphorus lone pair.[1,2,3] Unfortunately, thermally induced ROP does not permit molecular weight control, and well-defined polymers must be synthesized *via* living anionic polymerization, a painstaking synthetic technique. Ideally, transition-metal catalyzed ROP reactions, using capping agents to control molecular weight,[4] would be used to generate suitably tractable polymers, a process presenting much less of a synthetic challenge. The versatility of this approach has been demonstrated for a number of silicon-bridged ferrocenophanes, where access to both block copolymers and poly(silaferrocenes) with comb and star architectures has been possible.[5] As expected, however, the P(III)-bridged [1]ferrocenophanes do not undergo transition-metal catalyzed ROP, presumably because the lone pair on phosphorus binds strongly to the catalyst's metal centre.

We have previously reported that reaction of a P(III)-bridged [1]ferrocenophane with methyl triflate led to a phosphonium-bridged system (**7**) that did undergo transition-metal catalyzed ROP.[6] The work presented herein is part of an investigation into whether the phosphorus lone pair could be protected to allow a formally P(III)-bridged ferrocenophane to be polymerized using transition-metal catalysts. This approach has the advantage that subsequent deborylation of the poly(ferrocenylphosphine) borane adduct should be possible, for example by reaction with amines, thus providing a route to controlled molecular weight poly(ferrocenylphosphines).

Results and discussion

Addition of boranes (BX_3, X = H, Cl) to **1** at reduced temperatures led to quantitative formation of the corresponding borane adducts of **1**. In particular, mixing THF solutions of $BH_3 \cdot THF$ and **1** at 0 °C led (see Scheme 1) to the formation of **2**. Similarly, adding a heptane solution of BCl_3 to a CH_2Cl_2 solution of **1** at −40 °C led to the formation of **3**. Reaction progress can be readily monitored *via* ^{31}P NMR, as reactant and product resonances may be distinguished both from their positions and multiplicity.

The ^1H and ^{13}C NMR spectra of **1**, **2** and **3** are featurally very similar, the most striking exception being the broad 1 : 1 : 1 : 1 quartet of the borane hydrogens in the proton spectrum of **2**. In all the ^1H NMR spectra, the Cp ligands give rise to four resonances, because the phosphorus bridge is asymmetric relative to a plane containing itself and the Cp *ipso*-carbons. An atypical feature in the spectrum of **2** is the coincidence of the resonances due to the phenyl group's *meta* and *para* position hydrogens, whereas in the other systems

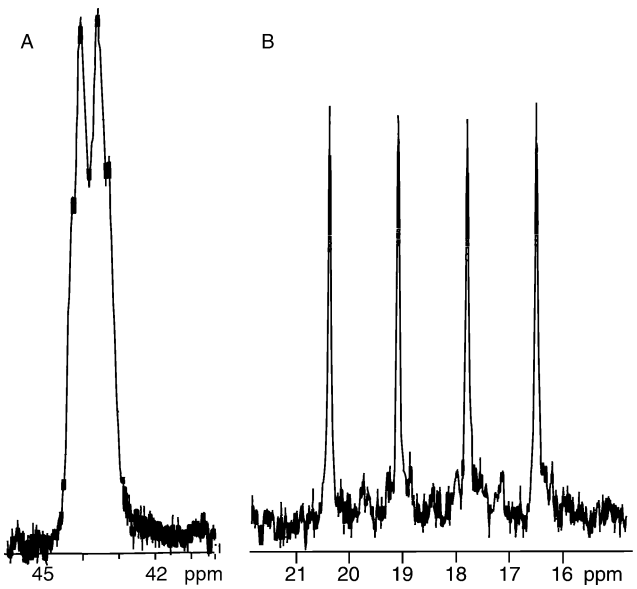

Fig. 1 ^{31}P solution NMR spectra: (A) **2** in CH_2Cl_2, (B) **3** in CD_2Cl_2.

three distinct resonances are seen for each phenyl group's hydrogens. A very clean doublet of doublet of doublets is observed for the *ortho* position hydrogens of **2**, exhibiting $^{3}J_{PH} = 12$ Hz, $^{3}J_{HH} = 7.5$ Hz and $^{4}J_{HH} = 1.85$ Hz.

In the ^{13}C NMR spectra, the position of the *ipso*-carbons was the most variable feature, becoming increasingly shielded as the phosphorus' substituent became increasingly electron-withdrawing. Thus, the position of the phenyl *ipso*-carbon's resonance shifts from 138 ppm for **1** to 129 ppm for **2** to 121 ppm for **3**. Similarly, the cyclopentadienyl *ipso*-carbon's resonance shifts from 18.5 ppm for **1** to 16.3 ppm for **2** to near 10 ppm for **3**.[7]

Although the ^{1}H and ^{13}C NMR spectra were useful in determining the identity of the products **2** and **3** as being [1]metallocenophanes, the most useful nuclei for differentiating the various compounds were, as expected, ^{11}B and ^{31}P. The singlet ^{31}P NMR resonance of **1** (at *ca.* 10 ppm) became (see Fig. 1) a poorly resolved quartet (pseudo-quartet at *ca.* 43 ppm) in the case of **2**, and a well resolved quartet (at *ca.* 18 ppm with $^{1}J_{BP} = 157$ Hz) in the case of **3**. The presence of resonances in the ^{11}B NMR spectra of **2** and **3** (see Fig. 2) provides additional evidence of the formation of the adducts. The large boron–phosphorus coupling constant of **3** caused its ^{11}B NMR spectrum to consist of a well-resolved doublet whose value of $^{1}J_{PB}$ (154 Hz) is in close agreement with that obtained from the ^{31}P NMR spectrum. For **2**, in contrast, the value of $^{1}J_{BP}$ had to be estimated from the pseudo-quartet in the ^{31}P NMR spectrum, and does not agree with the value of $^{1}J_{PB} = 39$ Hz obtained from the ^{11}B NMR spectrum, which consists of an incompletely resolved doublet. This latter value should be considered to be closer to the correct magnitude of the phosphorus–boron coupling constant for **2**.

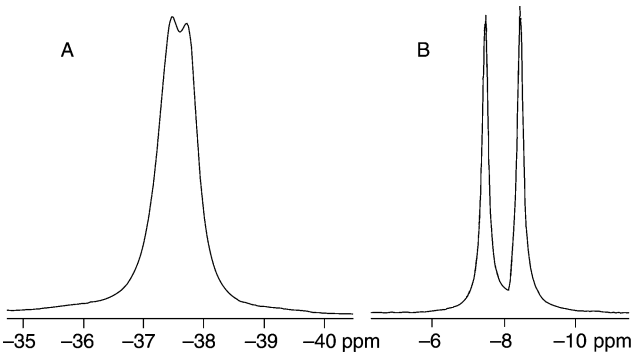

Fig. 2 ^{11}B solution NMR spectra: (A) **2** in $CDCl_3$, (B) **3** in CD_2Cl_2.

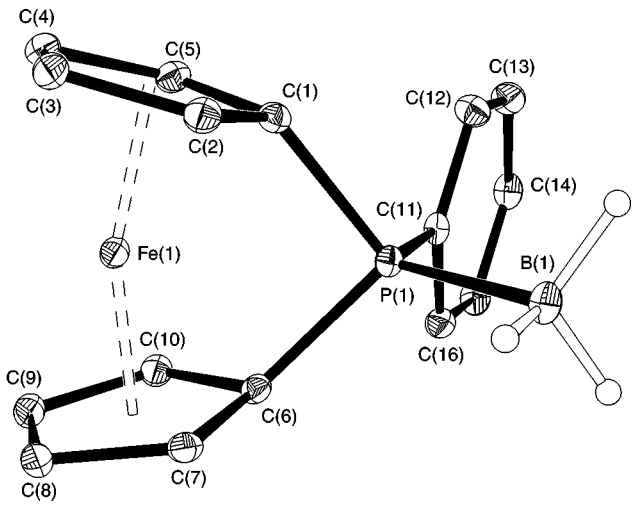

Fig. 3 ORTEP molecular structure diagram of **2** with thermal ellipsoids at 30% probability.

Crystals suitable for X-ray diffraction studies were obtained for both adducts, and ORTEP diagrams of **2** and $\mathbf{3}\cdot CH_2Cl_2$ are provided as Fig. 3 and 4, respectively. Table 1 contains pertinent crystal data and structural refinement information for these experiments. Bond lengths and selected angles have been provided in Tables 2 (for **2**) and 3 (for $\mathbf{3}\cdot CH_2Cl_2$). The structures of both adducts are consistent both with those of other phosphorus-bridged [1]ferrocenophanes, and with those of other borane adducts of tertiary phosphines. For example, the B–P bond length of $\mathbf{3}\cdot CH_2Cl_2$ [1.976(4) Å] is 0.059(6) Å longer than that of **2** [1.917(2) Å]. This compares with a difference of 0.056(12) Å between the B–P bond lengths of $Me_3P\cdot BCl_3$ [1.957(5) Å][8] and $Me_3P\cdot BH_3$ [1.901(7) Å].[9] The B–P bond lengths of both **2** and $\mathbf{3}\cdot CH_2Cl_2$ may be slightly (*ca.* 0.02 Å) longer than those of the corresponding Me_3P adducts, but the B–Cl bond lengths in both $\mathbf{3}\cdot CH_2Cl_2$ and the Me_3P adduct are similar (*i.e.* 1.850 Å).

A plane of symmetry in $\mathbf{3}\cdot CH_2Cl_2$ contains the iron atom, the bridging element (phosphorus), the boron atom, and the *ipso* and *para* carbons of the phenyl ring. There is, thus, no torsion angle between the Cp rings. This was also the case for the diphenylgermane-bridged [1]ferrocenophane, $[(\eta\text{-}C_5H_4)_2FeGePh_2]$,[10] but was not the case for the dimethylsilane-bridged [1]ferrocenophane, $[(\eta\text{-}C_5H_4)_2FeSiMe_2]$, which had a very small ring torsion [0.4(5)°].[11]

Both structures reveal ring-tilt angles, α, (see Fig. 5 for the definitions of the various angles in [1]metallocenophanes) consistent with other phosphorus-bridged [1]ferrocenophanes. The values of 24.38(10)° and 25.01(4)° for **2** and $\mathbf{3}\cdot CH_2Cl_2$, respectively, are somewhat smaller than the 26.7° observed in **1**, and similar to the value of 24.4(5)° observed for the P(v)-bridged (and cationic) compound **7**. If

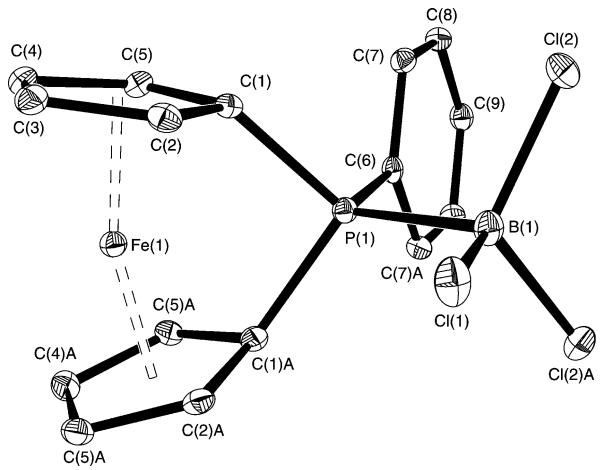

Fig. 4 ORTEP molecular structure diagram of $\mathbf{3}\cdot CH_2Cl_2$ with thermal ellipsoids at 30% probability. The solvent molecule has been omitted for clarity.

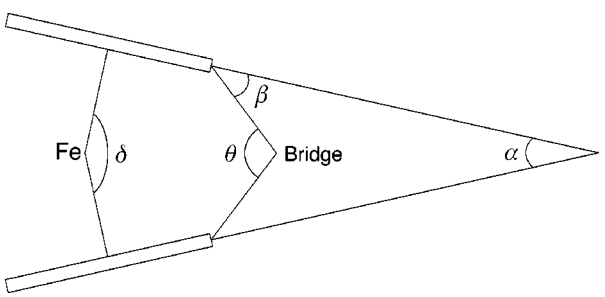

Fig. 5 Schematic defining the various angles of significance in a [1]ferrocenophane.

Table 1 Crystal data and structural refinement information for the X-ray structural determination of **2** and **3** · CH_2Cl_2

	2	**3** · CH_2Cl_2
Empirical formula	$C_{16}H_{16}BFeP$	$C_{17}H_{15}BCl_5FeP$
Formula weight	305.92	494.17
T/K	100.0(2)	100.0(1)
Crystal system	Triclinic	Orthorhombic
Space group	$P\bar{1}$	*Pnma*
a/Å	7.4376(3)	15.6327(3)
b/Å	8.9729(4)	11.9939(3)
c/Å	11.9365(5)	10.2391(6)
α/°	73.754(2)	90
β/°	83.435(2)	90
γ/°	66.728(2)	90
U/Å^3	702.56(5)	1919.80(13)
Z	2	4
μ/mm^{-1}	1.167	1.563
Reflections collected	6152	17120
Independent reflections	2843 [R(int) = 0.033]	2306 [R(int) = 0.080]
Final R indices [$I > 2\sigma(I)$]	$R_1 = 0.0282$, $wR_2 = 0.0731$	$R_1 = 0.0308$, $wR_2 = 0.0672$
R indices (all data)	$R_1 = 0.0328$, $wR_2 = 0.0764$	$R_1 = 0.0530$, $wR_2 = 0.0721$

the structures of these four compounds are compared, a trend of decreasing Fe–P separation and C_{ipso}–P bond length (see Table 4) with increasing electron deficiency at phosphorus is apparent. The longest bonds are those in **1**, with shorter bond lengths observed for **2**, **3** · CH_2Cl_2, and the shortest for **7**. The angles θ, β and δ are correspondingly smallest for **1** and largest for **7**. These trends are consistent with (but not proof of) an increasing bonding interaction between Fe and the bridging P as the positive character of the latter is increased. Such a trend has been commented on in previous work in which the Fe–P distance was observed before and after quaternization of the phosphorus centre either with sulfur[2] or methyl triflate[6] (to form **7**). In the former case, a decrease in the Fe–P distance of 0.096(4) Å was observed

Table 2 Bond lengths (Å) and selected angles (°) for **2** (ESDs in parentheses)

Fe(1)–C(1)	2.0004(18)	C(1)–C(5)	1.453(3)
Fe(1)–C(2)	2.0277(19)	C(2)–C(3)	1.430(3)
Fe(1)–C(3)	2.0856(19)	C(3)–C(4)	1.431(3)
Fe(1)–C(4)	2.0851(18)	C(4)–C(5)	1.424(3)
Fe(1)–C(5)	2.0320(18)	C(6)–C(10)	1.448(3)
Fe(1)–C(6)	1.9951(18)	C(6)–C(7)	1.452(3)
Fe(1)–C(7)	2.0258(18)	C(7)–C(8)	1.427(3)
Fe(1)–C(8)	2.0932(18)	C(8)–C(9)	1.430(3)
Fe(1)–C(9)	2.0983(19)	C(9)–C(10)	1.425(3)
Fe(1)–C(10)	2.0346(18)	C(11)–C(16)	1.398(3)
Fe(1)–P(1)	2.6847(5)	C(11)–C(12)	1.397(3)
P(1)–C(1)	1.8324(19)	C(12)–C(13)	1.390(3)
P(1)–C(6)	1.8276(18)	C(13)–C(14)	1.394(3)
P(1)–C(11)	1.8085(19)	C(14)–C(15)	1.390(3)
P(1)–B(1)	1.917(2)	C(15)–C(16)	1.392(3)
C(1)–C(2)	1.451(3)		
C(1)–P(1)–C(6)	96.06(8)	C(1)–P(1)–B(1)	114.11(9)
C(11)–P(1)–B(1)	115.49(9)	C(5)–C(1)–C(2)	106.34(16)
C(1)–P(1)–C(11)	107.12(8)	C(12)–C(11)–C(16)	119.91(17)

Table 3 Bond lengths (Å) and selected angles (°) for **3** · CH_2Cl_2 (ESDs in parentheses)

Fe(1)–C(1)	1.997(2)	Cl(2)–B(1)	1.850(2)
Fe(1)–C(2)	2.041(2)	C(1)–C(5)	1.451(3)
Fe(1)–C(3)	2.103(2)	C(1)–C(2)	1.454(3)
Fe(1)–C(4)	2.090(2)	C(2)–C(3)	1.422(3)
Fe(1)–C(5)	2.024(2)	C(3)–C(4)	1.428(4)
Fe(1)–P(1)	2.6464(9)	C(4)–C(5)	1.424(3)
P(1)–C(1)	1.812(2)	C(6)–C(7)	1.397(3)
P(1)–C(6)	1.796(3)	C(7)–C(8)	1.385(3)
P(1)–B(1)	1.976(4)	C(8) C(9)	1.389(3)
Cl(1)–B(1)	1.838(4)		
C(1)–P(1)– C(1)A	97.83(13)	C(5)–C(1)–C(2)	106.88(19)
C(6)–P(1)–B(1)	109.94(15)	C(7)–C(6)–C(7)A	119.9(3)
C(6)–P(1)–C(1)	108.81(9)	Cl(1)–B(1)–Cl(2)	111.03(14)
C(1)–P(1)–B(1)	115.36(10)		

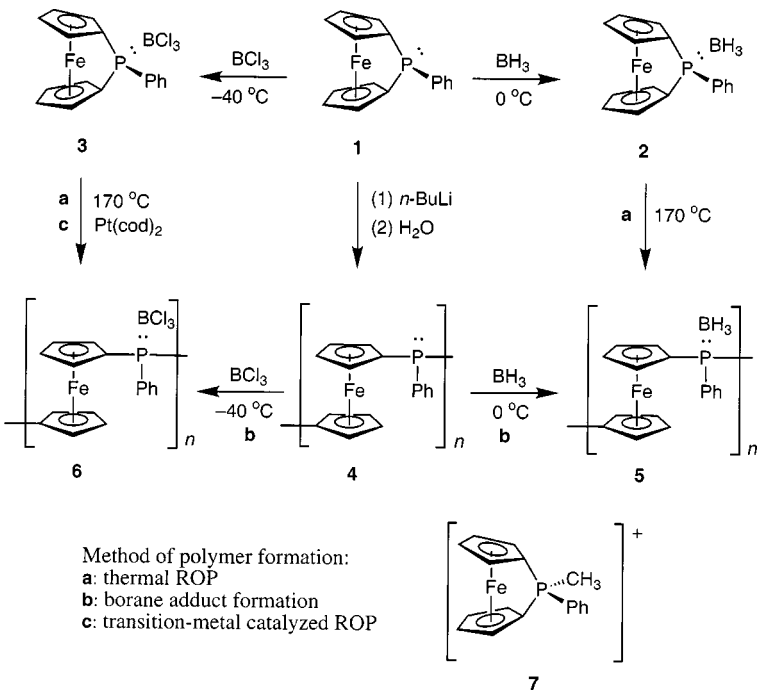

Scheme 1

between **1** and its sulfurized analogue (along with a shift in the ^{31}P resonance from 10 to 46 ppm) and, in the latter case, a decrease in Fe–P distance of 0.197(6) Å was observed between **1** and **7** (along with a shift in the ^{31}P resonance from 10 to 38 ppm). The changes in Fe–P distance between **1** and both **2** and **3**·CH_2Cl_2 are intermediate to these, with a decrease of 0.085(4) Å between **1** and **2** and of 0.128(4) Å between **1** and **3**·CH_2Cl_2. Somewhat surprising is the fact that the ^{31}P NMR resonance of **3** occurs at a higher field (19 ppm) than that of **2** (42 ppm). One would expect, using electronegativity arguments, BH_3 to be a weaker Lewis acid than BCl_3, and thus to have a less deshielding effect upon the phosphorus.[12] It has been previously noted, however, that BH_3 can behave as an anomalously strong acceptor towards phosphines (relative to haloboranes) compared to its behaviour towards amines.[8,12,13]

The UV–Vis data, however, do not seem to support BH_3 behaving as a stronger acceptor towards phosphines. For **1**,[14] **2** and **3** in CH_2Cl_2, the maxima of the lowest energy bands, similar to ferrocene's "band II", occur at 507, 499 and 494 nm, respectively. It appears, therefore, that as phosphorus is made more electron deficient, the band maximum shifts to higher energy. This is supported by the position of the band maximum for **7**, which occurs at 484 nm (in THF). While this datum cannot be exactly compared to the data obtained in CH_2Cl_2, it does clearly support the conclusion that the band maximum's position is related to the electronic environment of phosphorus. Such a conclusion must be treated with caution, however, since it is known that the energies of the significant orbitals are affected not only by the rings' substituents, but also by the magnitude of the tilt angle, α.[15]

Table 4 Selected bond lengths (Å) and angles (°) for a variety of phosphorus-bridged [1]ferrocenophanes. The definition of the various angles is given in Fig. 5. ESDs (where available) are given in parentheses after each value

	1	2	3·CH_2Cl_2	7
α	26.7	24.38(10)	25.01(4)	24.4(5)
β	32.5	36.0(1)	36.6(2)	37.9(4)
θ	90.6(3)	96.06(8)	97.83(13)	99.8(4)
δ	159.8	162.2(1)	162.2(1)	163.6(4)
Fe–P	2.774(3)	2.6847(5)	2.6464(9)	2.577(3)
C_{ipso}–P	1.842(13)	1.8300(19)	1.812(2)	1.772(10)
P–B	—	1.917(2)	1.976(4)	—

The thermal behaviour of **2** was examined by differential scanning calorimetry, and revealed a ROP exotherm centred at 166 °C, which integrated to 60 kJ mol^{-1}. This represents a lower limit to the energy released during thermal ROP, since no melt endotherm was apparent. Based on this information, thermal polymerization of **2** was effected in a sealed, evacuated Pyrex tube at 170 °C over 30 min. This resulted in an insoluble red–brown product, **5a**, which was characterized by pyrolysis-MS and solid state NMR. The pyrolysis-MS contained peaks consistent with the structure expected for the polymer. For example, peaks corresponding to ring-opened **1** [FcP(Ph)H, Fc = ferrocenyl] and cyclic dimers of **1** {[fcP(Ph)]$_2$, fc = ferrocenediyl} were observed. The MS of **2** does not result in the same fragmentation pattern, exhibiting a small molecular ion peak at 306, and peaks for **1** and the stepwise loss of CpH and Fe from **1**. This may be due in part to the fact that ionization of **2** was effected at a considerably lower temperature than that used for **5a**.

Solid-state CP-MAS NMR of **5a** revealed two broad peaks in the ^{13}C NMR spectrum, consistent with the Cp and phenyl regions. A non-quaternary suppression (NQS)[16] experiment revealed a quaternary carbon within the band envelope of each peak, also consistent with the presence of bound Cp and phenyl moieties. Singlet resonances were observed in the ^{31}P and ^{11}B solid-state NMR spectra at *ca.* 7 and *ca.* −40 ppm, respectively. Elemental analysis of **5a** could not, unfortunately, confirm the product's identity. The %C determined was more than 10% below the expected value, probably due to the formation of carbon-containing, combustion-resistant ceramics. The formation of such ceramics at elevated temperatures is known for ferrocene-containing polymers.[17]

In order to provide confirmation of the identity of **5a**, the borane adduct of **4** was synthesized. A sample of **4** [M_n = 19 000; polydispersity index (PDI) 1.14], obtained by anionic polymerization of **1**, was treated with BH_3 in THF at 0 °C in a manner similar to the synthesis of **2**. The yellow product, **5b**, afforded ^1H and ^{13}C NMR spectra consistent with formation of a borane adduct of **4**. For example, the *ipso*-carbons in **5b** are shielded by 8 (Ph) and 3 (Cp) ppm

from their positions in **4**.[18] Considering the corresponding monomers, the *ipso*-carbon resonances of **2** are shielded by 9 (Ph) and 1 (Cp) ppm relative to their positions in **1**. In the ^{1}H NMR spectrum of **5b**, the most significant feature is the broad peak associated with BH_3. The remainder of the proton spectrum is very similar in appearance to that of the sulfurized derivative of **4**,[2] as might be expected. Significantly, the ^{31}P NMR spectrum showed a singlet peak at 8 ppm, and the ^{11}B NMR spectrum a singlet peak at −40 ppm, as were observed for **5a**. The pyrolysis-MS of **5b** contains fragments such as FcP(Ph) and $[fcP(Ph)]_n$, $n = 2$–4.

The correspondence of the solid-state NMR and pyrolysis-MS data is highly suggestive that polymers **5a** and **5b** are the same species, and that the insolubility of **5a** is due either to a very high molecular weight or to some degree of crosslinking or to a combination of both these factors. Attempts to determine the molecular weight of **5b** by gel permeation chromatography (GPC) resulted in estimates of M_n of *ca.* 9000. This is about half the expected value, and may be due to interactions between the polymer and the column material. Polymer **4** itself does not elute from a GPC column due to such interactions, unless it has first been derivatized with sulfur to afford the analogous phosphine sulfide polymer.[2] The tail in the GPC trace of **5b** (which extends to M_n *ca.* 19 000), and the broad PDI (about 2), are suggestive of some polymer–column interactions that retard elution.

Attempts to polymerize **2** *via* transition-metal catalyzed ROP using $PtCl_2$, Karstedt's catalyst, $[Rh(cod)_2]OTf$ (cod = 1,5-cyclooctadiene), and $Pt(cod)_2$ met with limited success, typefied by extremely poor yields of dark, insoluble product. The transition-metal catalyzed ROP attempt on **3** with $Pt(cod)_2$, in contrast, resulted in a bright orange precipitate that was extracted with CH_2Cl_2, resulting in a tan solid (**6c**) which was further analyzed by solid-state NMR and pyrolysis-MS. As with **5a**, **6c** possessed two broad peaks in its ^{13}C NMR spectrum, corresponding to the Cp (70 ppm) and phenyl (130 ppm) carbons. The NQS experiment indicated quaternary carbons in the same regions, as expected. The ^{11}B NMR spectrum of **6c** consisted of a singlet at 0 ppm with a broad shoulder to high field, while the ^{31}P NMR spectrum contained two broad singlets at −15 and 35 ppm, with the latter being of much greater intensity. As in the case of **5a**, we wished to synthesize a soluble adduct of polymer **4** to provide comparative NMR data for **6c**. The BCl_3 adduct of **4**, **6b**, is, however, an insoluble yellow–orange solid. It was examined by solid-state NMR, and was found to exhibit two broad peaks in its ^{13}C NMR spectrum, at 75 and 135 ppm, which compare favourably to the positions of the analogous peaks observed for **6c** (at 70 and 130 ppm, respectively), considering the peak widths. In the NQS experiment on **6b**, a single quaternary carbon resonance was observed in the Cp region (at *ca.* 70 ppm), and two resonances due to quaternary carbons in the phenyl region (at *ca.* 128 and 133 ppm). Its ^{31}P NMR spectrum contains a single peak (at −15 ppm), but two peaks are seen in the ^{11}B NMR spectrum, at 2 and 8 ppm. The peak at 2 ppm shows a pronounced shoulder (at *ca.* 4 ppm), which is roughly consistent with the expected magnitude of B–P coupling. The reason why multiple boron and phenyl *ipso*-carbon resonances are observed (but a single phosphorus resonance) is not clear. Polymer **6a**, an insoluble purple–brown solid obtained in low yield from the thermal ROP of **3**, exhibited peaks in its ^{11}B and ^{31}P NMR spectra at 4 and −20 ppm, respectively, in excellent agreement with the data for **6b**.

The pyrolysis-MS data of **6a**, **6b** and **6c** were consistent with the NMR data. The fragmentation pattern of **6b** at 300 °C revealed peaks corresponding to BCl_3 (116) and BCl_2 (81), with no fragmentation of the polymer backbone being observed. At 550 °C, however, fragmentation of the backbone results in peaks due to CpH, P(Ph), FcH and/or Ph_2PH, FcP(Ph), fcPFc, $Fc_2P(Ph)$, and $[fcP(Ph)]_2$; a similar fragmentation pattern to that observed for **5a**. The pyrolysis-MS of **6c** contains many of the fragments observed for **6b**, but two large peaks unobserved in the MS of **6b** dominate the fragmentation pattern. The peaks at 376 and 309 may arise from fragmentation of the unidentified species responsible for the ^{31}P NMR resonance at 35 ppm. From the intensity of the fragments in the MS of **6c** associated with fragments observed for **6b**, we tentatively suggest that the product formed in the transition-metal catalyzed ROP of **3** is perhaps 20% poly(ferrocenylphenylphosphine trichloroborane). While the amount of product generated certainly indicates that a catalytic process is at work, it is clear that the reaction mechanism is dominated by processes other than the desired chain-growth polymerization. These may involve, for example, reactions with B–H or B–Cl bonds in the case of **2** and **3** respectively.

Conclusions

The phosphorus-bridged [1]ferrocenophane **1**, and the corresponding ring-opened polymer, **4**, readily form adducts with boranes BX_3 (X = H, Cl). The monomeric borane adducts (**2** and **3**) undergo thermal polymerization to yield products (**5a** and **6a**) spectroscopically consistent with **5b** and **6b**, the borane adducts of **4** with BH_3 and BCl_3, respectively. Attempts at transition-metal catalyzed ROP of **2** and **3** led to insoluble, poorly defined products. The reaction of **3** with $Pt(cod)_2$ led to the formation of a mixture of products, **6c**, due to a catalytic process. Comparison of spectral data of **6c** with that for **6b** suggests the presence of the ring-opened polymer derived from **3** in low yield.

Experimental

Materials and methods

All reactions involving monomer were carried out under nitrogen atmospheres using standard Schlenk techniques in conjunction with an Innovative Technologies drybox. THF and hexanes were distilled from Na, and CH_2Cl_2 was dried on a Grubbs-type[19] solvent purification system using A-2 alumina under a nitrogen atmosphere, and deoxygenated by three freeze-pump-thaw cycles. BH_3 (1 M in THF) and BCl_3 (1 M in heptane) were purchased from Aldrich and used as received. Compound **1** was prepared using a published procedure.[20] Polymer **4** [M_n = 19 000 (calcd 18 800); PDI 1.14] was prepared by living anionic ROP in triply distilled THF using *n*-BuLi (1.6 M in hexanes) as the initiator and degassed H_2O as the terminator.[1b]

GPC were obtained on a Waters 2690 liquid chromatograph equipped with a model 510 HPLC pump, a model U6K injector, Ultrastyragel columns with pore sizes of 10^3–10^5 Å, and a Waters 410 differential refractometer. The eluent was THF with a flow rate of 1.0 mL min^{-1}, and results are reported *vs.* polystyrene standards. The sample of **4** was first derivatized with sulfur in order to allow it to pass through the column. This methodology has been discussed elsewhere.[2]

Solution NMR spectra were obtained on a Varian Unity 500 spectrometer (^{1}H at 500.0 MHz, ^{11}B at 160.5 MHz), a Varian VXR 400 spectrometer (^{1}H at 400.0 MHz, ^{13}C at 100.6 MHz), or a Varian Gemini-300 spectrometer (^{31}P at 121.6 MHz). ^{1}H, ^{13}C and ^{31}P spectra were referenced to solvent. ^{11}B spectra were run unlocked, and the glass peak was removed using a 32 point backwards linear prediction on a basis of 512 points, using 16 coefficients. Chemical shifts are reported relative to TMS (^{1}H and ^{13}C), 85% H_3PO_4 (^{31}P), or $BF_3 \cdot O(Et)_2$ (^{11}B). Solid-state CP-MAS NMR spectra were obtained on a Bruker DSX-400 (^{13}C at 100.6 MHz) or Bruker

DSX-200 (^{11}B at 64.2 MHz, ^{31}P at 81.0 MHz) spectrometers and were referenced to adamantane (^{13}C, 38.4 ppm *vs.* TMS), 85% H_3PO_4 (^{31}P), or $NaBH_4$ [^{11}B, −42.0 ppm *vs.* $BF_3 \cdot O(Et)_2$].[21] The ^{11}B NMR spectra of the samples containing BCl_3 were run as 90°-τ-180° spin-echo experiments, where τ is one rotor period.

Mass spectrometry was performed on a Micro Mass 70S-250 mass spectrometer in electron impact mode at 70 eV. Ionization was achieved thermally at *ca.* 200 °C for **2** and **3**, using a temperature ramp of 0.5 °C s^{-1} from *ca.* 40 to 533 °C for **5a**, discretely at 300 and 550 °C for **6a** and **6b**, and discretely at 200 and 550 °C for **5b** and **6c**. Differential scanning calorimetry was performed on a Perkin–Elmer DSC-7 calibrated to cyclohexane and indium. A heating rate of 10 °C min^{-1} was used between 40 and 200 °C. UV–Vis spectroscopy was obtained in CH_2Cl_2 on a Perkin–Elmer Lambda900 UV/Vis/NIR spectrometer. Elemental analysis was performed by Quantitative Technologies Inc., Whitehouse, NJ.

X-Ray crystallography data were collected on a Nonius Kappa CCD diffractometer using graphite monochromated Mo-Kα radiation ($\lambda = 0.71073$ Å). A combination of 1° phi and omega (with kappa offsets) scans were used to collect sufficient data. The data frames were integrated and scaled using the Denzo-SMN package.[22] The structures were solved and refined using the SHELXTL\PC v5.1 package.[23] Refinement was by full-matrix least-squares on F^2 using all data (negative intensities included). Hydrogen atoms were included in calculated positions.

CCDC reference number 440/176. See http://www.rsc.org/suppdata/nj/b0/b000935k/ for crystallographic files in .cif format.

Syntheses

***P*-Phenylphospha[1]ferrocenophane borane (2).** Compound **1** (222 mg, 0.760 mmol, FW 292.10) was dissolved in THF (3 mL), cooled in an ice bath, and borane (0.84 mL, 1 M in THF, 1.1 equiv.) was added slowly. The solution was allowed to stir for several minutes, and an aliquot was removed to determine reaction progress. 100% conversion (by ^{31}P NMR) was observed with the first aliquot (removed after 25 min.); hexanes (5 mL, *ca.* 2 equiv. v/v with THF) were added to the solution, which was then cooled to −20 °C for 2 h, resulting in orange–red crystals suitable for X-ray diffraction analysis. An isolated yield of 89% was obtained after drying overnight *in vacuo* at ambient temperature (206 mg, 0.673 mmol, FW 305.93). ^{1}H (400.0 MHz, $CDCl_3$, 293 K) δ 1.0 (br 1 : 1 : 1 : 1 q, $^1J_{BH}$ = *ca.* 100 Hz, BH_3), 4.33 (s, Cp, 2 H), 4.56 (s, Cp, 2 H), 4.60 (s, Cp, 2 H), 4.92 (s, Cp, 2 H), 7.55 (m, Ph, 3 H), 7.82 (m, Ph, 2 H); ^{1}H (400.0, MHz, C_6D_6, 293 K) δ 1.95 (br q, $^1J_{BH}$ = 97 Hz, av., BH_3), 3.81 (s, Cp, 2 H), 4.09 (s, Cp, 2 H), 4.15 (s, Cp, 2 H), 4.88 (s, Cp, 2 H), 7.32 (m, Ph, 3 H), 7.60 (ddd, $^3J_{PH}$ = 12 Hz, $^3J_{HH}$ = 7.5 Hz, $^4J_{HH}$ = 1.9 Hz, Ph-*ortho*, 2 H). Note: the 'singlets' observed for the Cp resonances in C_6D_6 were actually finely split multiplets ($J \leqslant 1$ Hz). ^{13}C (100.6 MHz, $CDCl_3$, 293 K) δ 16.3 (d, $^1J_{PC}$ = 32 Hz, *ipso*-Cp), 76.0 (s, Cp), 76.4 (d, $^2J_{PC}$ = 18 Hz, Cp), 79.4 (d, $^3J_{PC}$ = 5 Hz, Cp), 79.7 (d, $^2J_{PC}$ = 9 Hz, Cp), 128.5 (d, $^1J_{PC}$ = 61 Hz, *ipso*-Ph), 129.2 (d, $^2J_{PC}$ = 10 Hz, Ph), 130.6 (d, $^3J_{PC}$ = 10 Hz, Ph), 131.5 (d, $^4J_{PC}$ = 2 Hz, Ph). Note: *n* of the various $^nJ_{PC}$ were assigned with the assumption that the magnitude of *J* decreases as *n* increases. Quaternary carbons were assigned on the basis of intensity. ^{11}B (160.5 MHz, $CDCl_3$, 293 K) δ −37.5 (d, $^1J_{PB}$ = 39 Hz). ^{31}P (121.55 MHz, $CDCl_3$, 293 K) δ 42.6 (d, $^1J_{BP}$ = 58 Hz). DSC (10 °C min^{-1}) 60 kJ mol^{-1} ROP exotherm (onset 164 °C, peak 166 °C). UV–Vis (CH_2Cl_2) λ_{max} 499 nm, ε_{499} = 5.04 ± 0.08 × 10^2 L mol^{-1} cm^{-1}. Pyrolysis-MS (*ca.* 200 °C, EI, 70 eV) *m*/*z* (%) 56 (15) Fe, 170 (19) [226 − Fe], 226 (37) [292 − CpH], 292 (100) fcP(Ph) (fc = ferrocenediyl), 306 (2) fcP(Ph)·BH_3, 584 (32) $[fcP(Ph)]_2$. Elem. anal. calcd (%): C, 62.82; H, 5.27; Found (%): C, 62.21; H, 5.19.

***P*-Phenylphospha[1]ferrocenophane trichloroborane (3).** Compound **1** (497 mg, 1.70 mmol, FW 292.10) was dissolved in CH_2Cl_2 (10 mL), cooled to −40 °C, and trichloroborane (1.8 mL, 1 M in heptane, 1.06 equiv.), also at −40 °C, added quickly. Precipitate formation was noted immediately, and the reaction mixture was left overnight at −40 °C. The supernatant liquor was decanted, the product dissolved in a minimum of CH_2Cl_2 (15–20 mL) and recrystallized overnight (again at −40 °C), resulting in the formation of orange–red crystals (**3**·CH_2Cl_2) suitable for X-ray diffraction analysis. The product was dried *in vacuo* at ambient temperature for 3 h and was isolated in 84% yield (587 mg, 1.43 mmol, FW 409.27). ^{1}H (500.0 MHz, CD_2Cl_2, 293 K) δ 4.38 (s, Cp, 2 H), 4.74 (s, Cp, 2 H), 4.84 (s, Cp, 2 H), 5.43 (s, Cp, 2 H), 7.66 (s, Ph, 2 H), 7.78 (s, Ph, 1 H), 7.99 (s, Ph, 2 H). ^{13}C (100.6 MHz, CD_2Cl_2, 293 K) δ 10.6 (d, $^1J_{PC}$ = 33 Hz, *ipso*-Cp), 77.5 (d, J_{PC} = 14 Hz, Cp), 77.7 (s, Cp), 81.1 (d, J_{PC} = 7 Hz, Cp), 82.4 (d, J_{PC} = 8 Hz, Cp), 121.2 (d, $^1J_{PC}$ = 69 Hz, *ipso*-Ph), 129.7 (d, $^2J_{PC}$ = 11 Hz, Ph), 133.8 (d, $^3J_{PC}$ = 9 Hz, Ph), 134.1 (d, $^4J_{PC}$ = 2 Hz, Ph). ^{11}B (160.5 MHz, CD_2Cl_2, 293 K) δ −8.0 (d, $^1J_{PB}$ = 154 Hz). ^{31}P (121.6 MHz, CD_2Cl_2, 293 K) δ 18.5 (q, $^1J_{BP}$ = 157 Hz). UV–Vis (CH_2Cl_2) λ_{max} 494 nm, ε_{494} = 4.33 ± 0.06 × 10^2 L mol^{-1} cm^{-1}. Pyrolysis-MS (*ca.* 200 °C, EI, 70 eV) *m*/*z* (%) 56 (18) Fe, 81 (26) BCl_2, 170 (22) [226 − Fe], 226 (42) [292 − CpH], 292 (100) fcP(Ph), 328 (23) FcP(Ph)Cl (Fc = ferrocenyl). Elem. anal. cald (%): C, 46.96; H, 3.20. Found (%): C, 46.99; H, 3.16.

Thermal polymerization of 2 to give poly-*P*-phenylphospha[1]ferrocenophane borane (5a). Compound **2** (150 mg, 0.490 mmol, FW 305.93) was sealed into an evacuated Pyrex tube and placed in a polymerization oven at 170 °C for 30 min. The cooled tube was opened under inert atmosphere. The red–brown product, **5a**, was obtained quantitatively, and found to be essentially insoluble in all solvents. (In CH_2Cl_2, $CHCl_3$ and THF a slight colouration of the solvent was observed.) Solid-state NMR: ^{13}C (100.6 MHz, 293 K) δ 70 (s, Cp, 1.7 kHz), 130 (s, Ph, 2 kHz). ^{11}B (64.2 MHz, 293 K) δ −42 (s, 2.2 kHz). ^{31}P (81.0 MHz, 293 K) δ 7.9 (s, 350 Hz). Pyrolysis-MS (T_{max} = 533 °C, EI, 70 eV) *m*/*z* (%) 66 (35) CpH, 121 (45) CpFe, 186 (100) ferrocene and/or Ph_2PH, 294 (52) FcP(Ph)H, 584 (32) $[fcP(Ph)]_2$. Elem. anal. calcd (%): C, 62.82; H, 5.27. Found (%): C, 52.05; H, 4.97.

Poly-*P*-phenylphospha[1]ferrocenophane borane (5b). Polymer **4** (100 mg, M_n = 19 000, PDI = 1.14) was dissolved in THF (7 mL), cooled in an ice bath and borane (0.6 mL, 1 M in THF, 1.8 equiv.) was added slowly. The solution was warmed to room temperature, allowed to stir overnight, concentrated to *ca.* 4 mL, and was added dropwise to hexanes (100 mL) with vigorous stirring. The solid was redissolved in THF (1 mL), reprecipitated by dropwise addition into rapidly stirred hexanes, collected by vacuum filtration and dried overnight *in vacuo* at 35 °C. While the reaction appeared quantitative by ^{31}P NMR, the isolated yield of yellow polymer was 78 mg (74%). ^{1}H (400.0 MHz, CD_2Cl_2, 293 K) δ 1.12 (br s BH_3), 3.8–4.5 (m, Cp, 8 H), 7.43 (s, Ph, 2 H), 7.48 (s, Ph, 1 H), 7.66 (s, Ph, 2 H). ^{13}C (75.5 MHz, CD_2Cl_2, 293 K) δ 73.0 (d, $^1J_{PC}$ = 68 Hz, *ipso*-Cp), 73.2 (d, J_{PC} = 8 Hz, Cp), 73.8 (d, J_{PC} = 12 Hz, Cp), 73.9 (d, J_{PC} = 5 Hz, Cp), 74.8 (d, J_{PC} = 6 Hz, Cp), 128.8 (d, J_{PC} = 9 Hz, Ph), 130.8 (s, *ipso*-Ph), 131.6 (s, Ph), 132.5 (d, J_{PC} = 9 Hz, Ph). ^{11}B (160.5 MHz, CD_2Cl_2, 293 K) δ −40 (s). ^{31}P (121.6 MHz, CD_2Cl_2, 293 K) δ 7.7 (s). GPC M_n = 9000; PDI = 1.94. These GPC data should be

considered to be inaccurate, as interactions between the analyte and the column material have likely skewed the results. Pyrolysis-MS (550 °C, EI, 70 eV) *m/z* (%) 78 (72) PhH, 108 (66) P(Ph), 186 (62) FcH and/or Ph_2PH, 293 (29) FcP(Ph), 400 (8) fcPFc, 478 (12) $Fc_2P(Ph)$, 584 (31) $[fcP(Ph)]_2$, 876 (4) $[fcP(Ph)]_3$, 1168 (0.5) $[fcP(Ph)]_4$.

Thermal polymerization of 3 to give poly-*P*-phenylphospha[1]ferrocenophane trichloroborane (6a). Compound **3** (200 mg, 0.489 mmol, FW 409.27) was heated to 170 °C for 30 min. under a nitrogen atmosphere. No melting of the solid was observed, although a colour change from orange–red to purple–brown occurred. The resultant solid was extracted with 1.5 mL aliquots of CH_2Cl_2 until the extracts were colourless. After drying *in vacuo* the product **6a** (36 mg, 18%) was characterized by ^{11}B and ^{31}P NMR spectroscopy. Solid-state NMR: ^{11}B (64.2 MHz, 293 K) δ 4 (s, 1.1 kHz). ^{31}P (81.0 MHz, 293 K) δ −20 (s, 2.5 kHz). Pyrolysis-MS (550 °C, EI, 70 eV) *m/z* (%) 66 (64) CpH, 78 (100) PhH, 108 (52) P(Ph), 186 (75) FcH, 293 (1) FcP(Ph).

Poly-*P*-phenylphospha[1]ferrocenophane trichloroborane (6b). Polymer **4** (67 mg, $M_n = 19\,000$, PDI = 1.14) was dissolved in CH_2Cl_2 (7 mL), cooled to −40 °C, and trichloroborane (0.25 mL, 1 M in heptane, 1.1 equiv., also at −40 °C) was added. A bright yellow–orange precipitate formed immediately. The colourless supernatant was decanted, and the precipitate was rinsed with a small volume of CH_2Cl_2 (resulting in a colourless supernatant liquor) prior to being dried *in vacuo* for 2 h at 35 °C, to yield 62 mg (66%) of a bright yellow–orange powder (insoluble in hexanes, toluene, dichloromethane and THF). Solid-state NMR: ^{13}C (50.3 MHz, 293 K) δ 75 (s, Cp, 1.3 kHz), 135 (s, Ph, 1.1 kHz). ^{11}B (64.2 MHz, 293 K) δ 2 (s, 450 Hz), 8 (s, 350 Hz). ^{31}P (81.0 MHz, 293 K) δ −15 (s, 1.1 kHz). Pyrolysis-MS (300 °C, EI, 70 eV) *m/z* (%) 81 (100) BCl_2, 116 (35) BCl_3; (550 °C, EI, 70 eV) *m/z* (%) 66 (100) CpH, 108 (54) P(Ph), 186 (91) FcH, 293 (25) FcP(Ph), 400 (19) fcPFc, 478 (13) $Fc_2P(Ph)$, 584 (9) $[fcP(Ph)]_2$.

Reaction of 3 with $Pt(cod)_2$ to give poly-*P*-phenylphospha[1]ferrocenophane trichloroborane (6c). A solution of compound **3** (200 mg) in CH_2Cl_2 (12 mL) was treated with $Pt(cod)_2$ (12 mg, 6 mol %), and stirred for 48 h, resulting in the precipitation of a bright orange product. The yellow–orange supernatant was decanted, and the product was rinsed with hexanes and dried *in vacuo* for 2 h. The solid residue was extracted 5 times with 1.5 mL aliquots of CH_2Cl_2 (until the supernatant liquors were colourless), and the insoluble tan product (147 mg, 74%) was dried *in vacuo* for 2 h at 35 °C. Solid-state NMR: ^{13}C (100.6 MHz, 293 K) δ 70 (s, Cp, 2 kHz), 130 (s, Ph, 2 kHz). ^{11}B (64.2 MHz, 293 K) δ 0 (s, 1.5 kHz). ^{31}P (81.0 MHz, 293 K) δ 35 (s, 2 kHz), −15 (s, 2 kHz). Pyrolysis-MS (200 °C, EI, 70 eV) *m/z* (%) 173 (100) CpPhPH, 238 (54) $Cp_2P(Ph)$, 294 (9) FcP(Ph)H, 328 (31) FcP(Ph)Cl; (550 °C, EI, 70 eV) *m/z* (%) 66 (30) CpH, 121 (34) CpFe, 186 (100) FcH and/or Ph_2PH, 262 (21) unassigned, 294 (13) FcP(Ph)H, 309 (53) unassigned, 376 (41) unassigned, 400 (3) fcPFc, 478 (4) $Fc_2P(Ph)$.

Acknowledgements

C. E. B. E. and I. M. thank the Natural Sciences and Engineering Research Council of Canada for financial support. We are also grateful to Alex Young for the mass spectral measurements and to Karen Temple for the DSC data.

Notes and references

1 (*a*) C. H. Honeyman, T. J. Peckham, J. A. Massey and I. Manners, *Chem. Commun.*, 1996, 2589; (*b*) T. J. Peckham, J. A. Massey, C. H. Honeyman and I. Manners, *Macromolecules*, 1999, **32**, 2830.
2 C. H. Honeyman, D. A. Foucher, F. Y. Dahmen, R. Rulkens, A. J. Lough and I. Manners, *Organometallics*, 1995, **14**, 5503.
3 For previous studies of the catalytic applications of poly(ferrocenylphosphines) formed by condensation routes, see J. D. Fellman, P. E. Garrou, H. P. Withers, D. Seyferth and D. D. Traficante, *Organometallics*, 1983, **2**, 818.
4 P. Gómez–Elipe, P. M. Macdonald and I. Manners, *Angew. Chem., Int. Ed. Engl.*, 1997, **36**, 762.
5 P. Gómez–Elipe, R. Resendes, P. M. Macdonald and I. Manners, *J. Am. Chem. Soc.*, 1998, **120**, 8348.
6 T. J. Peckham, A. J. Lough and I. Manners, *Organometallics*, 1999, **18**, 1030.
7 The numbers reported for the Cp *ipso*-carbon must be treated with caution as the peaks were ill-resolved, with an extremely poor signal-to-noise ratio. The peaks observed at *ca.* 10 ppm do not, however, appear to be artifacts.
8 D. L. Black and R. C. Taylor, *Acta Crystallogr., Sect. B*, 1975, **31**, 1116.
9 P. S. Bryan and R. L. Kuczkowski, *Inorg. Chem.*, 1972, **11**, 553.
10 H. Stoeckli–Evans, A. G. Osborne and R. H. Whiteley, *J. Organomet. Chem.*, 1980, **194**, 91.
11 W. Finckh, B.-Z. Tang, D. A. Foucher, D. B. Zamble, R. Ziembinski, A. Lough and I. Manners, *Organametallics*, 1993, **12**, 823.
12 *Comprehensive Coordination Chemistry*, ed. G. Wilkinson, Pergamon Press, Oxford, UK, 1987, vol. 3, ch. 24.
13 J. Apel and J. Grobe, *Z. Anorg. Allg. Chem.*, 1979, **453**, 28.
14 UV–Vis data for **1** in CH_2Cl_2 has not been published elsewhere: λ_{max} 507 nm, $\varepsilon_{494} = 4.38 \pm 0.05 \times 10^2$ L mol^{-1} cm^{-1}.
15 (*a*) S. Barlow, M. J. Drewitt, T. Dijkstra, J. C. Green, D. O'Hara, C. Whittingham, H. H. Wynn, D. P. Gates, I. Manners, J. M. Nelson and J. K. Pudelski, *Organometallics*, 1998**17**, 2113; (*b*) J. C. Green, *Chem Soc. Rev.*, 1998, **27**, 263; (*c*) A. Berenbaum, H. Braunschweig, R. Dirk, U. Englert, J. C. Green, F. Jäkle, A. J. Lough and I. Manners, *J. Am. Chem. Soc.*, in press
16 S. J. Opella and M. H. Frey, *J. Am. Chem. Soc.*, 1979, **101**, 5854.
17 B.-Z. Tang, R. Petersen, D. A. Foucher, A. Lough, N. Coombs, R. Sodhi and I. Manners, *J. Chem. Soc., Chem. Commun.*, 1993, 523.
18 ^{13}C (75.5 MHz, CD_2Cl_2, 293 K) data for **4** has not been published elsewhere: δ 71.8 (s, Cp), 72.5 (s, Cp), 73.0 (d, $J_{PC} = 12$ Hz, Cp), 74.1 (d, $J_{PC} = 12$ Hz, Cp), 78.9 (d, $^1J_{PC} = 5$ Hz, *ipso*-Cp), 128.2 (d, $J_{PC} = 7$ Hz, Ph), 129.2 (s, Ph), 134.3 (d, $J_{PC} = 22$ Hz, Ph), 139.5 (d, $^1J_{PC} = 10$ Hz, *ipso*-Ph).
19 A. B. Pangborn, M. A. Giardello, R. H. Grubbs, R. K. Rosen and F. J. Timmers, *Organometallics*, 1996, **15**, 1518.
20 D. Seyferth and H. P. Withers, Jr., *Organometallics*, 1982, **1**, 1275.
21 R. K. Harris, J. Bowles, I. R. Stephenson and E. H. Wong, *Spectrochim. Acta, Part A*, 1988, **44**, 273.
22 Z. Otwinowski and W. Minor, *Methods Enzymol.*, 1997, **276**, 307.
23 G. M. Sheldrick, *SHELXTL\PC*, v5.1, Bruker Analytical X-ray Systems, Madison, WI, USA, 1997.